



HAL
open science

MODELING CONVECTIVE DRYING OF FOOD PRODUCTS UNDER LARGE DEFORMATION

Bianca Cristine Marques, Artemio Plana-Fattori, Carmen Cecilia Tadini,
Denis Flick

► **To cite this version:**

Bianca Cristine Marques, Artemio Plana-Fattori, Carmen Cecilia Tadini, Denis Flick. MODELING CONVECTIVE DRYING OF FOOD PRODUCTS UNDER LARGE DEFORMATION. 11th International Conference on Simulation and Modelling in the Food and Bio-Industry (FOODSIM'2020), Sep 2020, Gand, Belgium. hal-03080722

HAL Id: hal-03080722

<https://hal.science/hal-03080722>

Submitted on 17 Dec 2020

HAL is a multi-disciplinary open access archive for the deposit and dissemination of scientific research documents, whether they are published or not. The documents may come from teaching and research institutions in France or abroad, or from public or private research centers.

L'archive ouverte pluridisciplinaire **HAL**, est destinée au dépôt et à la diffusion de documents scientifiques de niveau recherche, publiés ou non, émanant des établissements d'enseignement et de recherche français ou étrangers, des laboratoires publics ou privés.

MODELING CONVECTIVE DRYING OF FOOD PRODUCTS UNDER LARGE DEFORMATION

Bianca Cristine Marques (1,2), Artemio Plana-Fattori (3,*), Carmen Cecilia Tadini (1,2), and Denis Flick (3)

(1) University of São Paulo, Escola Politécnica, Chemical Engineering Department,
Main Campus, Butantã, 05508-010 São Paulo, SP, Brazil

(2) University of São Paulo, FoRC/NAPAN Food Research Center

(3) Université Paris-Saclay, INRAE, AgroParisTech, UMR SayFood, 91300 Massy, France

(* author corresponding address:

AgroParisTech, Dept. MMIP, 16 rue Claude Bernard, 75231 Paris CEDEX 5

E-mail: artemio.planafattori@agroparistech.fr

KEYWORDS

food drying, shrinkage, large deformation

ABSTRACT

A novel approach for modeling the convective drying of cylindrical slices of food products whose dehydration occurs under large deformation is proposed. The model considers heat and mass transfer phenomena as well as the volume decrease (shrinkage). Instead using a complex thermo-hygro-mechanical model, an original geometrical approach is used to determine local shrinkage. When drying starts, shrinkage occurs in the direction normal to the surface, which corresponds to the direction of moisture gradient; later on, shrinkage becomes isotropic. The food matrix is represented by a 2D axis-symmetrical domain. The finite volume method is used, and the mesh boundaries move with the dry-matter. Simulations considered thermo-physical properties of *yacon* (*Smallantus sonchifolius*) slices, for which the volume is divided by about 10 during drying. The model reproduced a shrinkage behavior which is intermediate between the hypothetical cases of constant aspect ratio and constant surface area for the food matrix.

INTRODUCTION

Solid and semi-solid food systems are highly heterogeneous materials that may be considered as consisting of a three-dimensional solid network holding large quantities of a liquid phase, very often an aqueous solution. Dehydration of foods is one of the most common processes used to improve food stability: it decreases considerably the water activity of the material, which reduces microbiological activity and then minimizes physical and chemical changes during its storage. The demand of high-quality products in the food market requires dehydrated foods that maintain at a high level the nutritional and sensorial properties of the fresh product. The understanding of the factors responsible for the

decrease in the quality of the product during the dehydration process is thus of major relevance. One of the most important physical changes that the food suffers during drying is the reduction of its volume. Loss of water and heating cause stresses in the cellular structure of the food leading to change in shape and decrease in dimension (Mayor and Sereno, 2004).

A complete thermo-hygro-mechanical model requires, in addition to thermal conductivity and water diffusivity, the knowledge of rheological parameters (Young's modulus, Poisson's coefficient, contraction coefficient due to water loss...). Moreover, especially under large deformation, the food material cannot be considered as purely elastic; plastic or visco-elastic behavior, with additional parameters, should be taken into account. All these mechanical parameters depend on temperature and water content, and are difficult to measure or estimate (e.g., Curcio and Aversa, 2014).

Here we present a simple numerical model for studying the evolution of food products which can experience significant shrinkage under drying. Only geometrical assumptions are made about shrinkage, and the detailed mechanical behavior of the food material is ignored. Classical approaches for heat and mass transfer are used (see for instance Silva Jr. *et al.*, 2019). The original contribution lies in the geometrical considerations for estimating how shrinkage is distributed in different directions.

The approach is illustrated for a cylindrical slice of *yacon* (*Smallantus sonchifolius*), a plant cultivated originally in South America for its tuberous, mildly sweet roots. The interest on *yacon* has increased (Caetano *et al.*, 2016); it constitutes a good option for low-carbohydrate diets because its low amounts of sucrose and glucose and high amount of non-digestible carbohydrates.

In parallel to the implementation of the numerical model, these authors are studying the convective drying of slices of *yacon* with the help of a pilot drier unit, as well as estimating thermo-physical properties. The experimental work already done is summarized in a companion article (Marques *et al.*, 2020).

NOMENCLATURE

a_w	water activity [dimensionless]
Bi	Biot number [dimensionless]
$C, K, X_{w,m}$	parameters in GAB model
$C_{sat}\{T\}$	saturated water vapor concentration at temperature T [kg-w-m ⁻³]
C_{dm}^*	dry-matter <u>intrinsic</u> heat capacity [J/kg-dm/K]
C_w^*	Water <u>intrinsic</u> heat capacity [J/kg-w/K]
D	diffusivity of water in the food product [m ² ·s ⁻¹]
h	convective heat transfer coefficient [W·m ⁻² ·K ⁻¹]
\vec{j}_q	energy flux [J·m ⁻² ·s ⁻¹]
$\vec{j}_{w/dm}$	Water flux relative to the dry-matter [kg-w·m ⁻² ·s ⁻¹]
k	mass transfer coefficient [m·s ⁻¹]
r, z	radial and axial position [m]
R, Z	radius and thickness of a food slice [m]
RH	air relative humidity [dimensionless]
S	(total) surface of the food matrix [m ²]
t	time [s]; drying starts at $t = 0$
T	temperature [K]
u	food internal energy [J/kg-dm]
u_{dm}	dry-matter internal energy [J/kg-dm]
u_w	water internal energy [J/kg-w]
\vec{v}_{dm}	dry-matter velocity in the food slice [m·s ⁻¹]
V	(total) volume of the food matrix [m ³]
X_w	water content in the food product, dry basis [kg-w/kg-dm]
\vec{Y}	displacement vector of dry-matter [m]
	GREEK SYMBOLS
λ	food product thermal conductivity [W·m ⁻¹ ·K ⁻¹]
ΔH_v	latent heat of water vaporization [J·kg ⁻¹]
ΔS	cross-section surface of a cell [m ²]
ΔV	volume of a cell [m ³] containing a constant mass of dry-matter
Δz	height of a cell [m]
ρ_{dm}	dry-matter mass density [kg-dm·m ⁻³]
ρ_{dm}^*	dry-matter <u>intrinsic</u> mass density [kg·m ⁻³]
ρ_w^*	water <u>intrinsic</u> mass density [kg·m ⁻³]
τ	surface-drying characteristic time [s]
	SUBSCRIPTS
a, dm, w	Air, dry-matter, water
0	initial (when drying starts)

ASSUMPTIONS AND GOVERNING EQUATIONS

The convective drying of a slice of food matrix is hereafter studied by taking into account the following assumptions:

- evaporation occurs at the surface only;
- liquid water migrates inside the product relatively to dry matter following moisture gradient;
- no porosity appears during drying (i.e. locally, the volume is entirely occupied by water and dry matter); and
- energy transfer occurs due to heat conduction and water convection.

The conservation equation for the dry-matter mass can be expressed by studying the evolution of its density:

$$\frac{\partial \rho_{dm}}{\partial t} + \vec{\nabla} \cdot \rho_{dm} \vec{v}_{dm} = 0, \quad (1)$$

wherein ρ_{dm} is expressed in kg of dry-matter by cubic meter of food product; the inverse of ρ_{dm} is the volume which contains one unit mass (1 kg) of dry-matter.

The conservation equation for the water content (dry basis) can be expressed, in its convective form, as:

$$\frac{\partial X_w}{\partial t} + \vec{v}_{dm} \cdot \vec{\nabla} X_w = \frac{1}{\rho_{dm}} \vec{\nabla} \cdot \vec{j}_{w/dm}; \quad (2)$$

wherein the water flux relative to the dry-matter is given by:

$$\vec{j}_{w/dm} = -D \vec{\nabla} (\rho_{dm} X_w). \quad (3)$$

Equation (2) is solved by taking into account the following boundary condition:

$$\vec{j}_{w/dm} \cdot \vec{n} = k (a_w C_{sat}\{T\} - RH C_{sat}\{T_a\}). \quad (4)$$

Finally, the total volume occupied by the food matrix containing 1 kg of dry matter can be expressed as the sum of volumes occupied by dry-matter and water:

$$\frac{1}{\rho_{dm}} = \frac{1}{\rho_{dm}^*} + \frac{X_w}{\rho_w^*}. \quad (5)$$

The internal energy of the food (by kg of dry-matter) is the sum of the internal energies of dry-matter and water:

$$u = u_{dm} + X_w u_w = (C_{dm}^* + X_w C_w^*) T, \quad (6)$$

its conservation equation can be expressed as:

$$\frac{\partial u}{\partial t} + \vec{v}_{dm} \cdot \vec{\nabla} u = \frac{1}{\rho_{dm}} (\vec{\nabla} \cdot \vec{j}_{w/dm} u_w + \vec{\nabla} \cdot \vec{j}_q), \quad (7)$$

where the energy flux is given by:

$$\vec{j}_q = -\lambda \vec{\nabla} T. \quad (8)$$

Equation (7) is solved by taking into account the following boundary condition:

$$\vec{j}_q \cdot \vec{n} = h (T - T_a) + \Delta H_v \vec{j}_{w/dm} \cdot \vec{n}. \quad (9)$$

The mass (k) and heat (h) transfer coefficients are correlated by the Lewis analogy.

The displacement vector of dry-matter \vec{Y} and its velocity \vec{v}_{dm} are related to the variation of dry-matter density:

$$\vec{v}_{dm} = \frac{d\vec{Y}}{dt} \quad (10)$$

$$\vec{\nabla} \cdot \vec{v}_{dm} = \frac{d}{dt} \left(\frac{1}{\rho_{dm}} \right) / \frac{1}{\rho_{dm}} . \quad (11)$$

Under small deformation we can express:

$$\vec{\nabla} \cdot \vec{Y} = 1 - \frac{1/\rho_{dm}}{1/\rho_{dm,0}} . \quad (12)$$

When dehydration is limited near to the matrix surface, the direction of shrinkage can be assumed parallel to the diffusion vector:

$$t < \tau \quad \frac{\partial}{\partial z} (\vec{v}_{dm,z}) / \frac{\partial}{\partial r} (\vec{v}_{dm,r}) = \vec{j}_{w/dm,z} / \vec{j}_{w/dm,r} . \quad (13)$$

When dehydration reaches the matrix core, shrinkage can be assumed isotropic. In the case of axis-symmetrical geometry we can express that:

$$t > \tau \quad \frac{\partial}{\partial z} (\vec{v}_{dm,z}) / \frac{\partial}{\partial r} (\vec{v}_{dm,r}) = \frac{1}{2} . \quad (14)$$

The transition time (also called surface-drying characteristic time) between these regimes can be estimated from the characteristic diffusion time for a slab:

$$\tau = 0.1 \frac{Z_0^2}{D} . \quad (15)$$

NUMERICAL SOLVING

The food matrix was assumed to have initially a cylindrical shape, and was represented by a two-dimensional (2D) axis-symmetrical domain (Figure 1). The finite volume method was applied using cylindrical coordinates.

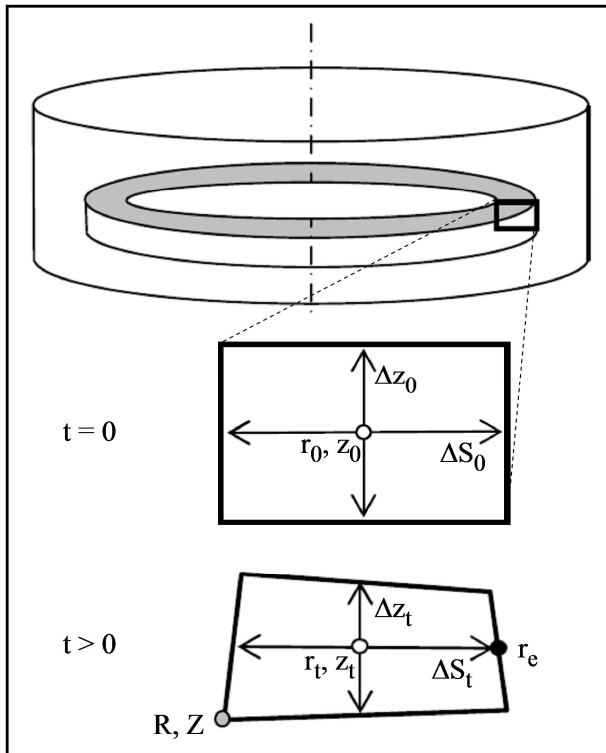


Figure 1: Schematic representation of the food matrix; and close-up view of an elementary cell at two instants.

Figure 1 includes close-up views of a control volume (cell). When drying starts ($t = 0$), the boundaries of the cell are regular and its initial volume ΔV_0 is given by multiplying its height Δz_0 and its cross-section surface ΔS_0 . Along the drying, boundaries move with the dry matter; as a result, cell position (r, z) as well as Δz_t and ΔS_t evolve. Hereafter we describe the shrinkage approach.

The cell volume can decrease in both radial and axial directions. At a given time $t > 0$, the volume ΔV of the cell at the position (r, z) is expressed from the mass conservation of dry-matter:

$$\Delta V_t \approx \Delta S_t \Delta z_t = \Delta S_0 \Delta z_0 \left(\frac{\rho_{dm,0}}{\rho_{dm,t}} \right) , \quad (16)$$

where the volume of food product containing 1 kg of dry-matter at this position at the time t is given by:

$$\frac{1}{\rho_{dm,t}} = \frac{1}{\rho_{dm}^*} + \frac{X_{w,t}}{\rho_w^*} . \quad (17)$$

It remains to evaluate how the volume decrease is distributed between the radial and axial directions.

At the very beginning of drying, the water content decreases near the surface; shrinkage is expected to occur mainly in the direction that is normal to the surface. This direction corresponds also to that of the moisture gradient.

The case of vertical gradient is schematized in Figures 2a and 2b. Evaporation at the horizontal surfaces affects more importantly the cell height Δz_t than the cell cross-section surface ΔS_t . The cell volume decrease can be estimated assuming vertical shrinkage only:

$$\Delta S_{t+\Delta t} \cong \Delta S_t \quad (18a)$$

$$\frac{(\Delta z_{t+\Delta t} - \Delta z_t)}{\Delta z_t} = \frac{(\Delta V_{t+\Delta t} - \Delta V_t)}{\Delta V_t} . \quad (18b)$$

Similar equations can be written for the case of horizontal gradient, associated with evaporation at vertical surfaces.

Later on during the drying, dehydration occurs also at inner parts of the food matrix. In the case of an isotropic material, shrinkage tends to be the same in all the directions.

Figures 2c and 2d put in evidence that the volume decrease occurs in both directions. In the 2D axis-symmetrical representation assumed for the food matrix, a given variation in the radial direction should be twice the corresponding variation in the axial direction:

$$\frac{(\Delta S_{t+\Delta t} - \Delta S_t)}{\Delta S_t} = \frac{2}{3} \frac{(\Delta V_{t+\Delta t} - \Delta V_t)}{\Delta V_t} \quad (19a)$$

$$\frac{(\Delta z_{t+\Delta t} - \Delta z_t)}{\Delta z_t} = \frac{1}{3} \frac{(\Delta V_{t+\Delta t} - \Delta V_t)}{\Delta V_t} . \quad (19b)$$

The behaviors expressed by equations (13, 14) can be combined to comply with the observed final shrinkage.

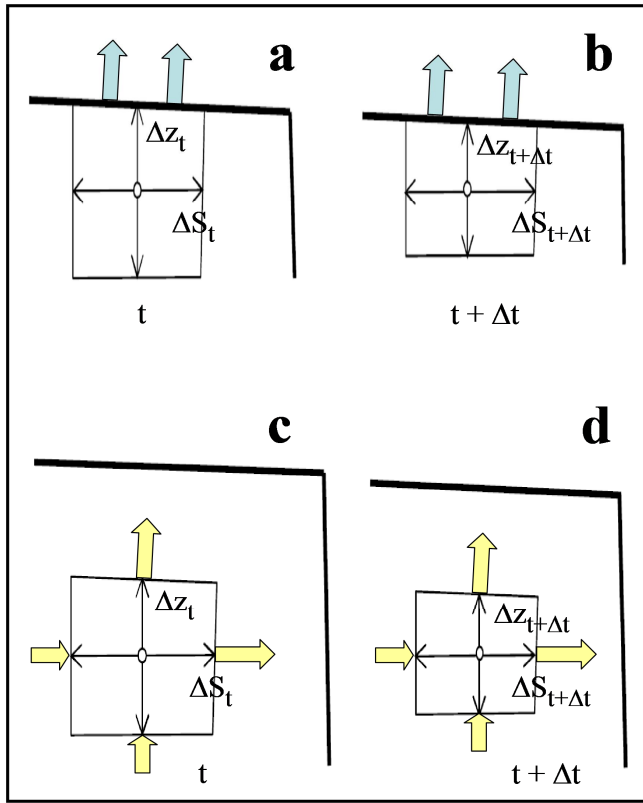


Figure 2: Schematic representation of shrinkage when drying starts: for cell volumes situated near the air-product interface (a, b), and for cell volumes situated inside the food matrix (c, d).

The approach described above was implemented in the programming language MATLAB (version R2016b; The MathWorks, Inc., Natick, Massachusetts, USA). No reasons forbid the use of other languages.

The 2D axis-symmetrical domain representing the food matrix was subdivided into rectangular cells; the mesh was built by considering 15 nodes in the radial direction and 8 in the axial direction.

The application of the boundary condition (4) requires the water activity at the surface of the slice. Experimental work has provided measurements of water content as a function of the water activity in slices of yacon (Figure 2c of Marques et al., 2020); those measurements were approximated by the Guggenheim-Anderson-deBoer (GAB) model:

$$X_w = \frac{C K X_{w,m} a_w}{(1 - K a_w)(1 - K a_w + C K a_w)}, \quad (20)$$

with parameters $C = 2.155$, $X_{w,m} = 0.136$ kg-w/kg-dm and $K = 1$. In the numerical model, water activity values were estimated at every position of the air-product interface through the GAB's inverse equation:

$$a_w = \frac{\beta - \sqrt{\beta^2 - 4(1-C)}}{2K(1-C)} \quad (21a)$$

$$\beta = 2 - (1 - X_{w,m}/X_w) C, \quad (21b)$$

taking into account predictions of the water content X_w at the previous time step.

Table: Key parameters considered in simulations.

air relative humidity	$RH = 20 \%$
air temperature	$T_a = 60 \text{ }^\circ\text{C}$
diffusivity of water in the product	$D = 3 \cdot 10^{-9} \text{ m}^2 \cdot \text{s}^{-1}$ (1)
dry-matter intrinsic mass density of the product	$\rho_{dm}^* = 1500 \text{ kg} \cdot \text{m}^{-3}$ (2)
initial height of the slice	$Z_0 = 0.007 \text{ m}$
initial radius of the slice	$R_0 = 0.02 \text{ m}$
initial temperature of the product	$T_0 = 20 \text{ }^\circ\text{C}$
initial water content in the product	$X_{w,0} = 10 \text{ kg-w/kg-dm}$
heat capacity of the product	$3500 \text{ J} \cdot \text{kg}^{-1} \cdot \text{K}^{-1}$ (2)
heat transfer coefficient	$h = 30 \text{ W} \cdot \text{m}^{-2} \cdot \text{K}^{-1}$
Thermal conductivity of the product	$\lambda = 0.5 \text{ W} \cdot \text{m}^{-1} \cdot \text{K}^{-1}$ (2)

(1) typical value for potatoes (Hassini et al., 2007)

(2) typical values for yacon (Marques et al., 2020)

Table 1 summarizes the key parameters used in studying the convective drying of slices of yacon over 4 hours. The heat transfer coefficient was assumed to be the same on all the air-product interfaces.

Figure 3a displays the food matrix before drying, at $20 \text{ }^\circ\text{C}$. Figures 3b and 3c present model predictions of the water content field at $t = 1.5$ h of drying, obtained after assuming that shrinkage follows the two above mentioned behaviors.

- On one hand, when the cell volumes are assumed to decrease following the moisture gradient only (Figure 3b), the food matrix rapidly deforms. This is because the volume decreases whereas the air-product interface area remains almost unchanged.
- On the other hand, when the cell volumes are assumed to decrease isotropically (Figure 3c), the radius of the upper and lower air-product interfaces decrease in an unrealistic manner.

Looking for a realistic shrinkage in the particular case of convective drying of yacon slices, the following strategy was adopted.

i) We started by estimating the surface-drying characteristic time through equation (15), after assuming that the diffusivity of water in the food matrix was to be about the same as for potatoes: we obtained $\tau \sim 27$ min.

ii) After these 27 minutes, shrinkage is assumed to be purely isotropic. Such a behavior is expressed by equation (14) and the cell volume decrease is computed by applying equations (19a, 19b).

iii) Along the 27 first minutes, shrinkage is assumed to be 50 % isotropic and 50 % driven by the moisture gradient. This behavior is intermediate to those expressed by equations (13, 14); the computation of the cell volume decrease combines equations (19a, 19b) with those for moisture-gradient-driven shrinkage.

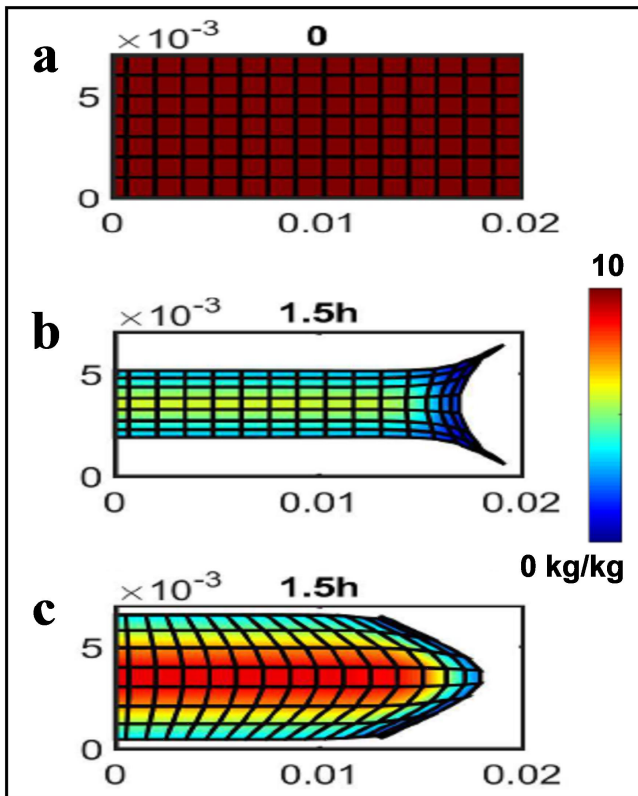


Figure 3: Water content fields: (a) before drying, (b) after 1.5h of drying, assuming that the cell volumes decrease according to the moisture gradient only, or (c) assuming that the cell volumes decrease isotropically.

RESULTS AND DISCUSSION

Figures 4 and 5 show respectively the temperature and the water content fields each 30 minutes, during which the food matrix was exposed to constant warm and dry air conditions (temperature 60 °C, relative humidity 20 %).

Until about one hour after drying starts, only the product near to the surface experiences dehydration and shrinkage: during this period, no dehydration occurs at the center of the slice and consequently no deformation is observed nearby. Later on, the whole food slice is dehydrated and therefore is affected by shrinkage. At the end of drying (after 4 h), the thickness as well as the radius are divided by about 2.2 and the volume by about 10. The final shape of the food slice includes the occurrence of 'horns' in the corners, which seems to be exaggerated. This could perhaps be corrected by limiting the cells stretching.

The temperature field is relatively homogeneous, especially at the beginning of drying. This can be explained by the low Biot number; when drying starts we have:

$$Bi = \frac{h(Z_0/2)}{\lambda} \approx 0.2 .$$

The temperature rapidly reaches the wet-bulb value (about 33 °C) and remains close to it until about 3 h, including near the surface. This can be explained by the fact that the diffusivity is high enough to ensure a water activity close to the unity at the surface. Later, when the surface becomes really dry ($X_w < 1$ kg-water/kg-dry-matter), the product temperature tends towards the dry air temperature (60 °C), especially near the corners.

Luyben et al. (1980) have studied the shrinkage behavior of different food materials under drying. In the case of tissue of fresh apples, those authors identified a first phase associated with homogeneous shrinkage, followed by rumpling but maintaining a constant surface area. Such a shrinkage behavior can be appreciated in Figure 2 of Bernstein and Norena (2014), who studied drying of small volumes of yacon. We may conclude that our numerical simulations are consistent in predicting the drying of a food matrix with relatively high water content.

Figure 6 summarizes the whole drying history of the food slice from model predictions.

Figures 6a and 6b show the evolution of temperature and water content at three selected positions of the food slice (see the encapsulated display in Figure 6a). Positions A and B move along the shrinkage history, being always located at the slice surface; they experience moisture gradients which are stronger than that at position C. During the first hour, positions A and B correspond to similar water content tendencies, while position C (at the slice center) is associated with negligible dehydration. Later on, drying effectively starts at position C, and becomes stronger at position B (between the corners) than at A.

Figure 6c displays the water activity at these three positions. Until about one hour after drying starts, the dehydration behavior is similar along the slice surface (positions A and B); later on, dehydration becomes faster between the corners (position B). At the slice center (position C), dehydration is negligible during the first two hours of drying, and later exhibits a parallel tendency to that experienced at the closest surface (position A).

Figure 6d shows that the volume decreases progressively by a factor of about 10, following a decreasing rate. During the first hour (surface drying and shrinkage), the slice thickness (Z) decreases faster than the top surface (which is proportional to R^2); later on, the trends are opposite.

Figure 6e shows that the drying rate decreases with time t i.e. with decreasing mean water content, Figure 6f. This is first due, during about the first 3 hours, to a decrease of the air-product interface area; after about 3 hours, the drying rate is additionally reduced because of the decrease of water activity at the surface.

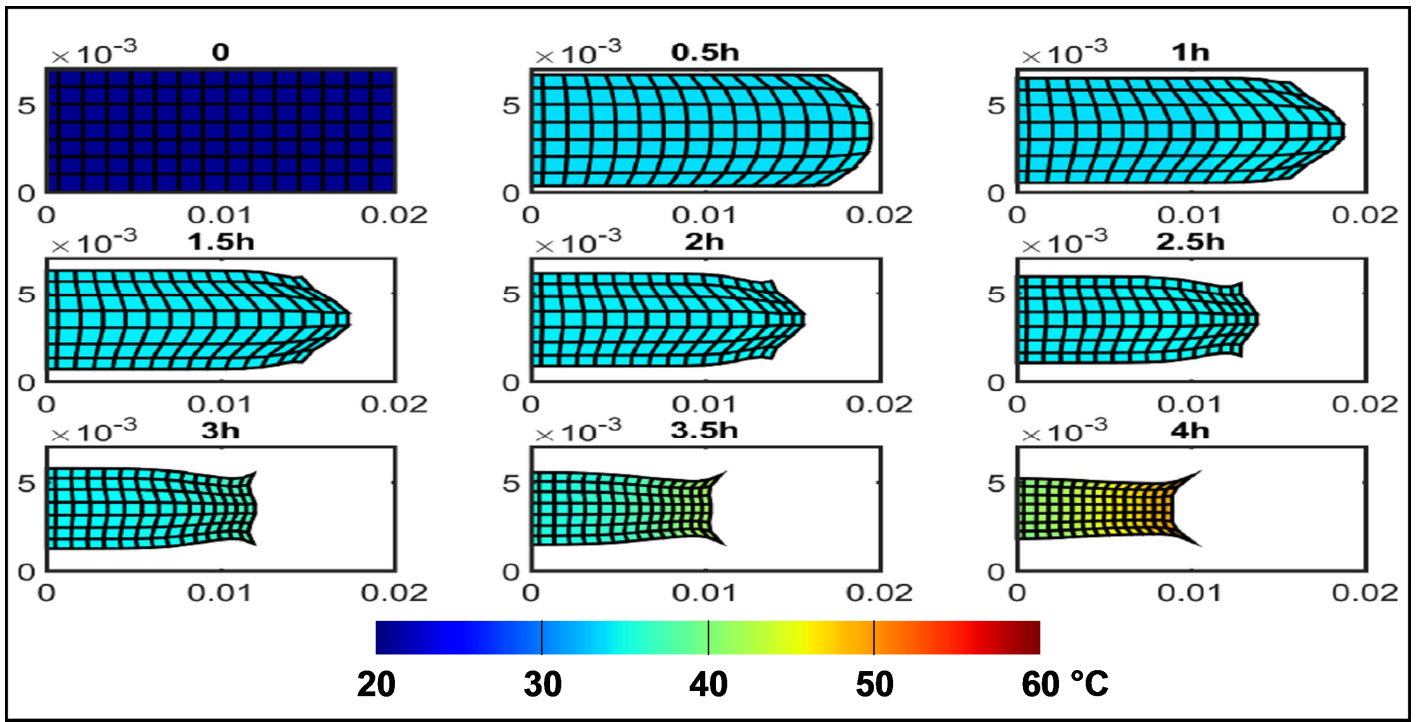


Figure 4: Temperature field in the food slice every 30 min; convective drying starts at $t = 0$. Dimensions of the food slice are expressed in meters.

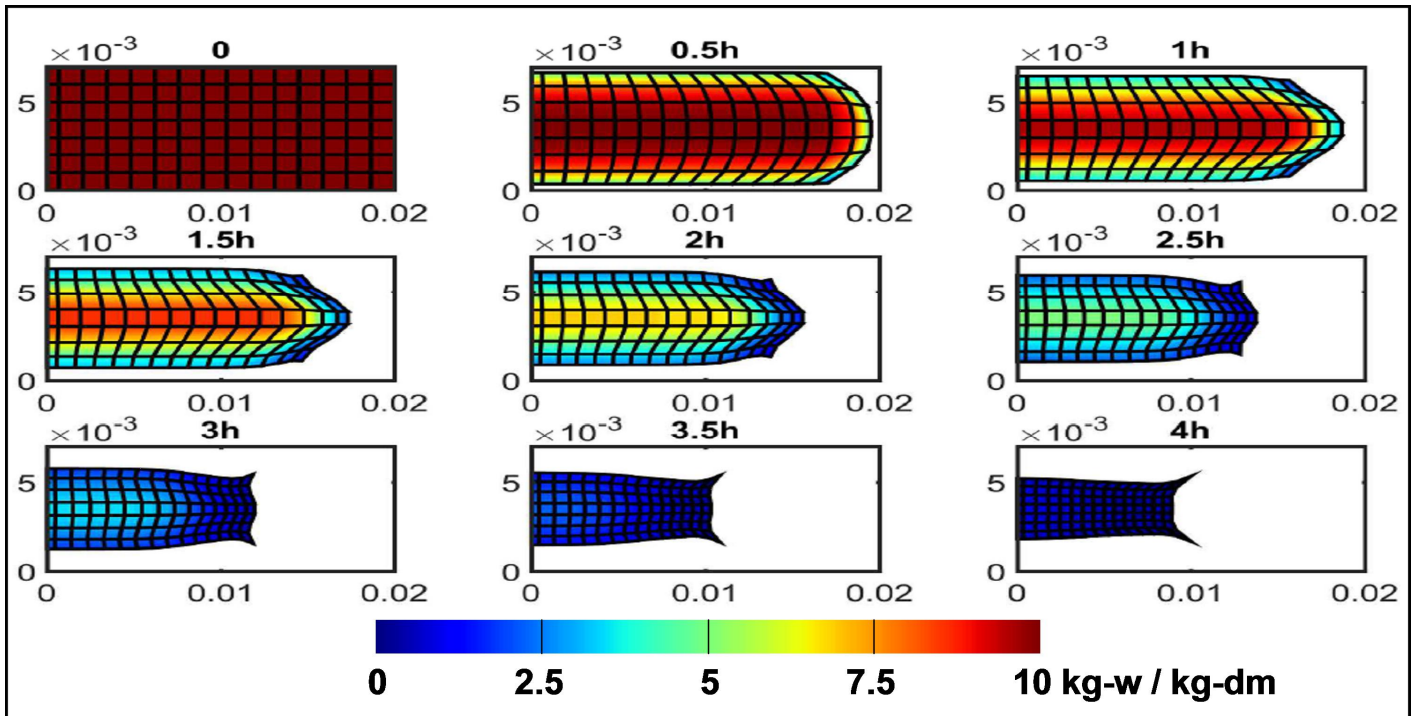


Figure 5: Water content field in the food slice every 30 min; convective drying starts at $t = 0$. Dimensions of the food slice are expressed in meters.

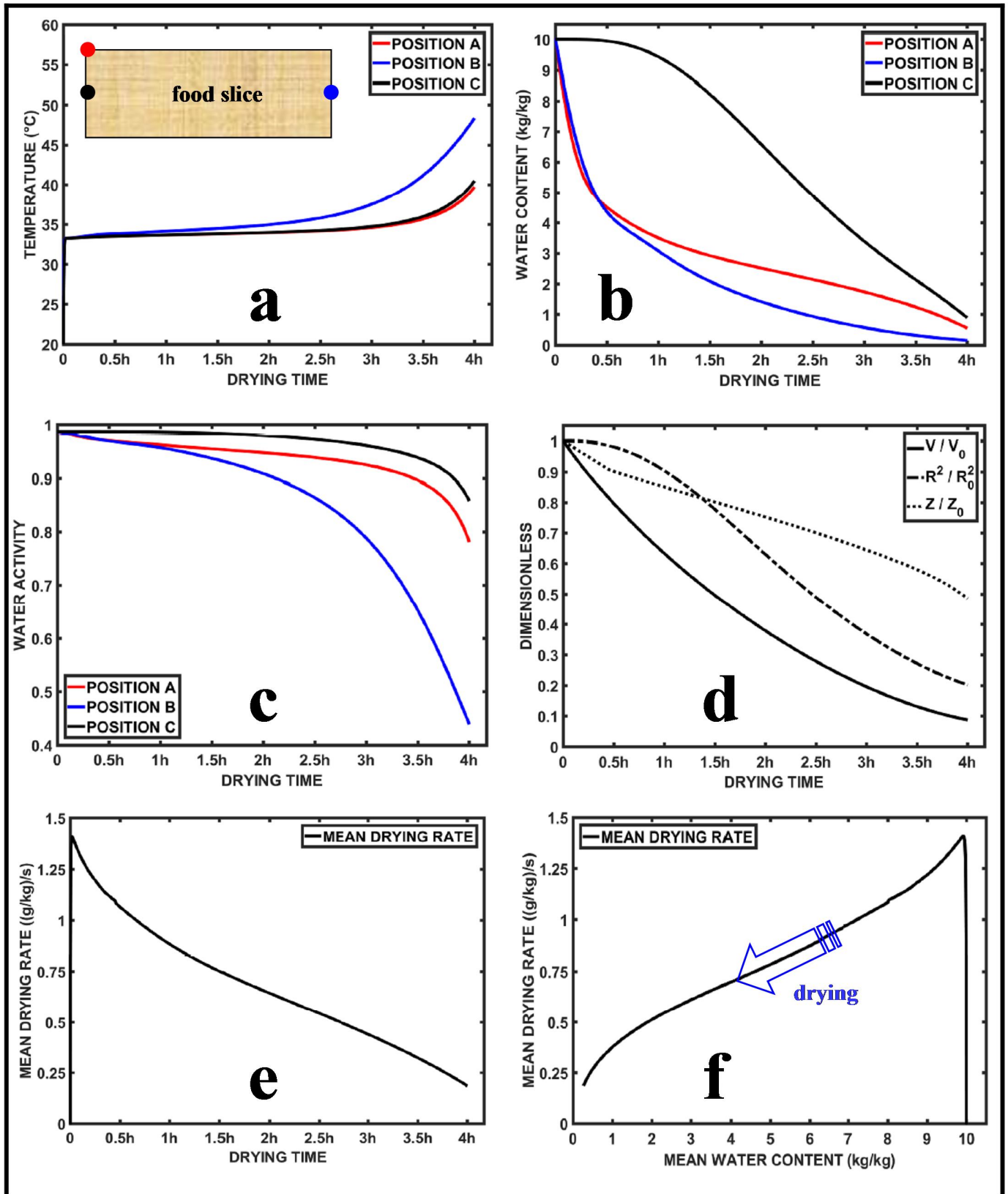


Figure 6: Drying history of the food slice as predicted by the numerical model: evolution of the temperature and of the water content at selected positions (displays **a** and **b**), bulk geometrical features as function of the drying time and of the mean water content (**c** and **d**), and mean drying rate as function of the drying time and of the mean water content (**e** and **f**).

CONCLUDING REMARKS AND FUTURE WORK

Drying phenomena (water migration inside the matrix, evaporation at its boundaries) cannot be dissociated from the geometrical evolution of the food matrix. For example, considering shrinkage normal to the product surface rather than isotropic leads to lower decrease of the air-product interface area, and therefore lower decrease of drying rate. A simple approach which does not require a complex mechanical model was proposed for shrinkage. The goal was to estimate how the local volume reduction (due to dehydration) is distributed between axial and radial shrinkage.

The proposed rule is that during superficial drying, shrinkage is rather normal to the surface and later becomes isotropic. The relative importance of these two behaviors might be assessed by monitoring the total surface S_t and volume V_t values for slices of the food product under consideration. The shape of the slices is expected to be preserved under isotropic shrinkage; at an instant t , we can write $S_t/S_0 = (V_t/V_0)^\alpha$ with $\alpha = 2/3$. On the other hand, under shrinkage driven by the moisture gradient only, the total surface of the food slice is expected to be preserved; such a situation corresponds to $\alpha = 0$ in the relationship above. Hence, the real behavior of the food matrix could be studied along the drying period.

Ongoing work includes:

- to take into account the influence of water content on the thermo-physical properties of *yacon* slices (mass density, heat capacity, thermal conductivity), as a way to assess the predictive potential of the numerical model under realistic conditions;
- to investigate the influence of the convective heat transfer coefficient applied as boundary condition at the air-product interfaces, including the adoption of different values at the three interfaces;
- to limit the stretching of the food matrix, as a way to reduce the occurrence of unrealistic geometrical features (such as the 'horns' at the corners).

In its present implementation, the approach was successfully applied for a case where the volume was divided by 10 during drying. The algorithm can be adapted, for instance, for including simple reaction kinetics, as a way to predict the influence of drying on chemical properties at different positions of the food matrix.

ACKNOWLEDGEMENTS

The research leading to these results received funding from grants 2018/21327-1, São Paulo Research Foundation (FAPESP), and 306414/2017-1, (Brazil) National Council for Scientific and Technological Development (CNPq).

REFERENCES

- Bernstein, A.; and Norena, C. P. Z. 2014. "Study of thermodynamic, structural, and quality properties of yacon (*Smallanthus sonchifolius*) during drying". *Food and Bioprocess Technology*, 7, 148-160.
- Caetano, B. F. R.; de Moura, N. A.; Almeida, A. P. S.; Dias, M. C., Sivieri, K.; and Barbisan, L. 2016. "Yacon (*Smallanthus sonchifolius*) as a food supplement: Health-promoting benefits of fructooligosaccharides". *Nutrients*, 8, 436.
- Cursio, S.; and Aversa, M. 2014. "Influence of shrinkage on convective drying of fresh vegetables: A theoretical model". *Journal of Food Engineering*, 123, 36-49.
- Hassini, L.; Azzouz, S.; Peczalski, R.; and Belghith, A. 2007. "Estimation of potato moisture diffusivity from convective drying kinetics with correction for shrinkage". *Journal of Food Engineering*, 79, 47-56.
- Luyben, K. C. A. M.; Olieman, J. J.; and Bruin, S. 1980. "Concentration dependent diffusion coefficients derived from experimental drying curves". In *Drying'80, Proceedings of the Second International Symposium* (Montreal, Canada, July 6-9, 1980). Hemisphere Pub. Corp., Washington D.C., U.S.A. volume 2, 233-243.
- Marques, B. C.; Plana-Fattori, A.; and Tadini, C. C. 2020. "Data acquisition for modelling convective drying of yacon (*Smallanthus sonchifolius*) slices". *11th International Conference on Simulation and Modelling in the Food and Bio-Industry (FOODSIM'2020)* (April 2020, Ghent, Belgium).
- Mayor, L.; and Sereno, A. M. 2004. "Modelling shrinkage during convective drying of food materials: A review". *Journal of Food Engineering*, 61, 373-386.
- Silva Jr., M. A. V.; Rabi, J. A.; Ribeiro, R.; and Dacanal, G. C. 2019. "Modeling of convective drying of cornstarch-alginate gel slabs". *Journal of Food Engineering*, 250, 9-17.

BIOGRAPHIES

BIANCA CRISTINE MARQUES is a Brazilian Ph.D. student in the Univ. of São Paulo, being advised by Carmen. As a part of her research, she is just joining AgroParisTech (Apr. 2020-2021); with Artemio and Denis, she will develop numerical models for studying the drying of *yacon*.

ARTEMIO PLANA-FATTORI was born in Brazil; he studied Atmospheric Sciences in the Univ. of Sao Paulo and later in the Univ. of Lille (Ph.D. in 1994). After 20 years teaching and conducting research in Brazil, he joined AgroParisTech in 2010, where he works with numerical modeling applied to food engineering.

CARMEN CECILIA TADINI conducts research on food science and engineering, with applications in pasteurization, bakery, drying and biodegradable films by extrusion. She is Full Professor at Univ. of São Paulo and author of one of the few textbooks about Food Engineering in Portuguese.

DENIS FLICK is Full Professor at AgroParisTech. He conducts research in modeling and numerical simulation of coupled phenomena in food processes (heat and mass transfer, fluid flow and product deformation, product transformation), with applications in food cold chain equipment, heat exchangers, cooking and baking, dairy products, bread, and ice cream. His teaching area includes transport phenomena, thermodynamics, and numerical modeling.